Open Access

Recent Progress in Materials

LIDSEN Publishing Inc.

Original Research

Green Synthesis of Metal-Organic Biohybrid (Mob) Nanomaterials

Navya Uppu [1, †], Kelly McMahen [1, †], Tasneem Khasru [1], Mark A. DeCoster [1, 2, *]

1. Louisiana Tech University, Biomedical Engineering, Ruston, Louisiana, USA; E-Mails: nup001@latech.edu; kam053@latech.edu; tkh013@latech.edu; decoster@latech.edu
2. Louisiana Tech University, Institute for Micromanufacturing, Ruston, Louisiana, USA

† These authors contributed equally to this work.

* **Correspondence:** Mark A. DeCoster; E-Mail: decoster@latech.edu

Academic Editor: Hossein Hosseinkhani

Special Issue: Green Synthesis of Nano Materials

Recent Progress in Materials
2022, volume 4, issue 4
doi:10.21926/rpm.2204020

Received: August 02, 2022
Accepted: October 13, 2022
Published: October 17, 2022

Abstract

Green synthesis of nanomaterials endeavors to reduce the use of high energy methods with those that may include lower temperatures and pressures, use of natural products, and bottom-up self-assembly. Here we describe the generation of metal-organic biohybrids (MOBs) with nanoscale features synthesized at physiological (37°C) and room temperature (25°C). These MOBs utilized the naturally occurring amino acid dimer cystine as the biological component, and a series of metals, including copper, silver, and cobalt. The copper- and silver- based nanomaterials generated were distinct in size and shape. Copper formed elongated high-aspect ratio structures which we have named CuHARS. In contrast, the self-assembly of cystine and silver formed nanoparticles which we designate as AgCysNPs, and cobalt formed particles which we designate as CoMOBs. Both cobalt and silver could be combined with copper in the same reaction vessel to carry out green synthesis of different nanomaterials simultaneously. Post-synthesis the polarization of light by CuHARS provided one measure to distinguish the size and shape of different MOBs generated simultaneously.

Keywords
Metal; copper; silver; cystine; cobalt

1. Introduction

We have previously described the self-assembly of MOBs with nano- and micro-scale features using the metals copper and silver [1]. Unique to our synthesis compared to many other nanomaterials is that copper and silver MOBs are synthesized at physiological temperature (37°C). This is a benefit for green nanomaterials synthesis, since the energy footprint for self-assembly processes at 37°C which we use, is much less than for many other reported green procedures which use elevated temperatures, often for extended periods of time [2, 3]. Other work for example has reported production of nanomaterials at room temperature, but use harsh chemicals [4] or top-down energy driven processes such as multiple grinding steps and sonication [5]. Other green synthesis methods for nanomaterials include the use of biological mediators such as bacteria and fungi [6, 7], or use natural materials such as plant extracts [8, 9]. These biological methods have benefits, but may also involve complex steps that could provide challenges for scaling up production. Further, due to variability in the growth and harvesting of the biological component (for example plant extracts), different synthesis batches might be expected to vary. In contrast, the single biological component we use in our green synthesis method is the natural amino acid dimer cystine [1, 10]. We isolated the pure, single component as essential to our green synthesis method, in a step-by-step elimination of all other factors isolated from cell culture conditions where the original discovery was made [10]. Thus, we can now generate nanomaterials using green synthesis and defined stoichiometry of metal or metal salts with the single biological component, cystine. This is done without the need of enzymes or microbes or other co-factors, which may be present when harvesting green components used from plant extracts or active bacteria or fungal preparations.

We consider the materials described here as biohybrids due to their stable incorporation of a biological component (cystine), and a non-biological metal such as copper (CuHARS) or silver (AgCysNPs). Key to our discovery of MOBs was the demonstration that CuHARS self-assembled from either copper nanoparticles or copper sulfate, yet both forms contained sulfur upon elemental analysis using EDX by scanning electron microscopy [10]. This finding indicated that the stable self-assembled CuHARS had incorporated sulfur from the cystine used during the synthesis, and/or from the monomer form of cystine, cysteine, which also contains sulfur.

Due to their differences in size and shape, the different MOBs using copper or silver (CuHARS and AgCysNPs, respectively), also offer different avenues for continued green synthesis directions post-synthesis. AgCysNPs remain as nano-scale colloids for long periods of time [1], which provides potential benefits for optics and coatings. However, it makes concentration of the material more difficult. In contrast, CuHARS settle rather quickly [1], without agglomeration, providing further green synthesis steps in the application of this material. Centrifugation may also be used to accelerate the process. Due to the very limited aggregation of CuHARS, the material may be separated by size by settling over time (or by centrifugation), and then easily dispersed almost instantaneously by vortexing or by simple inversion (mixing) of the material in water.

Finally, while we cannot yet control the size of CuHARs during synthesis, post-synthesis we can shift the average size to more nanoscale using sonication [10].

Since the MOBs that we have described are generated via a bottom-up, self-assembly process, consistency of temperature is a consideration, but to further explore the diversity and flexibility of our method, we compared green synthesis of MOBs here for the first time at 37°C vs 25°C. This consideration for green synthesis of nanomaterials at modest temperatures would be a beneficial driver when considering scaling up production of a material, since the range of manufacturing temperatures available between 37°C and 25°C could encompass large arrays of production vessels. Insight into these green synthesis methods could limit (or minimize) the need for synthesis ovens, and thus diminish the electricity footprint.

Another advantage to our described method of green synthesis is that the generation of MOBs is self-limiting. When stoichiometry and the environmental conditions are chosen correctly, CuHARS self-assemble in a self-limiting manner. The reaction to form CuHARS may thus be terminated by simply removing the reaction vessel from heat, and moving it to a cooler temperature such as refrigeration (4°C).

2. Materials and Methods

2.1 Materials

Copper (II) sulfate pentahydrate, cobalt (II) sulfate, and sodium hydroxide were from Sigma-Aldrich (St. Louis, MO). Cysteine hydrochloride monohydrate (catalogue# C6852) and L-cystine (catalogue# C7602) were both from non-animal sources and were used as prepared from Sigma-Aldrich. Silver sulfate was from Alfa Aesar (Haverhill, MA).

2.2 Methods

Generation of CuHARS. CuHARS were generated as previously described using [10] copper sulfate; synthesis was terminated by moving synthesis vessels to 4°C for long-term storage.

Spectrophotometry. A Beckman-Coulter DU800 spectrophotometer was used to scan the absorbance of samples from 200-800 nm (or as indicated) in a volume of 700 µl. Scanning in the ultraviolet region utilized quartz cuvettes. Both amino acids were solubilized at 7.29 mg per 100 µl of NaOH, and then 14 µl of the concentrated solution added to 7 ml of deionized, sterile water as per the conditions used for MOBs synthesis.

Generation of AgCysNPs. AgCysNPs were generated in a total volume of 7 ml in general following the procedure described to generate CuHARS [10] and including cystine, but replacing copper with a 2 mg/ml solution of silver sulfate. In some cases as indicated, a final concentration of 1 mM HCl was included in the synthesis vessel as previously described [1]. Silver solution was used in 2 parts (700 µl), or 3 parts (1,050 µl) of the total volume as indicated, and paired with 2 parts (14 µl), or 3 parts (21 µl) of cystine solution, respectively.

Generation of multiple MOBs simultaneously. In some cases as indicated, CuHARS and AgCysNPs, or CuHARS and cobalt MOBs (CoMOBs), were generated simultaneously. Generation of multiple MOBs types simultaneously was carried out in a total volume of 7 ml in general following the procedure described to generate CuHARS alone [10] and including cystine, but also including with copper, a 2 mg/ml solution of silver sulfate or cobalt sulfate, respectively.

Separation of AgCysNPs with centrifugation. An Eppendorf model 5804R centrifuge was used at 2,500 rcf for ten minutes to separate larger AgCysNPs (pellet) from smaller nanoparticles (supernatant), using 15 ml polystyrene tubes (Perfector Scientific, Atascadero, CA), as indicated. For spectrophotometry scanning of AgCysNPs, NPs were subjected to 3 cycles of centrifugation using 4 ml of deionized water with retention of the pellet, as indicated. Final pellet was then resuspended in 3.5 ml of deionized water and analyzed by spectrophotometry from 200-800 nm.

Coffee-ring formation. Four microliters of separated AgCysNPs or other materials as indicated were spotted onto a glass microscope slide, and dried at 50°C. Dried spots were then imaged for coffee-ring formation using an inverted Leica DMI6000 B microscope with Leica DFC500 color camera or an inverted Olympus IX51 microscope with Olympus DP71 camera as indicated.

Dynamic Light Scattering (DLS) measurements. DLS measurements were taken on a Malvern Zetasizer Nano ZS instrument and associated analysis carried out using Zetasizer software (Ver. 7.1). Samples were sonicated for 5 minutes using a Branson model 1800 sonicator before taking DLS measurements.

Scanning electron microscopy (SEM) imaging: Scanning Electron Microscopy (SEM, Hitachi, Japan), was carried out on samples using a Hitachi FESEM by drying samples onto silicon wafers and then carrying out microscopy at the indicated magnification. Energy dispersive X-ray spectroscopy (EDX) analysis was used to identify elemental components of the scanned nanomaterials.

Magnetic Susceptibility. A magnetic field was applied using one or two neodymium ring magnets (Applied Magnets, Plano, TX), as indicated. The measured average local magnetic field was 107 ± 16 mTesla on the large opening side of the magnet, and 150 ± 49 mTesla for the small opening side of the magnet as measured by an F.W. BELL Gauss/TeslaMeter (Model 5080).

3. Results

3.1 Green Synthesis of Silver Nanoparticles

We assessed the comparative generation of AgCysNPs at 37°C and 25°C, over a period of 5 hours. Substantial yield was achieved, with slight color variations observed for the colloidal nanoparticle suspensions (Figure 1).

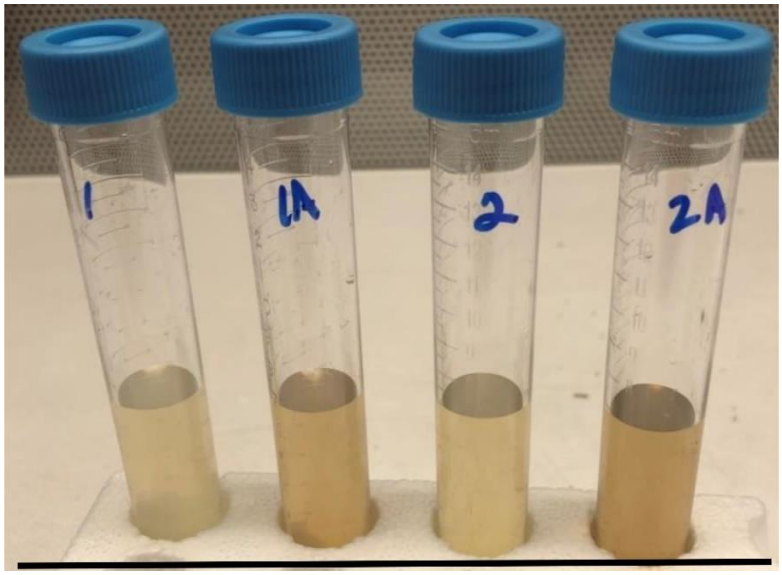

Figure 1 Colloidal solutions of AgCysNPs. As prepared AgCysNPs are shown in 15 ml tubes and were generated as shown from left to right under the following conditions: 1 = 37°C and 2parts Ag + 2parts Cys; 1A = 25°C and 2parts Ag + 2parts Cys; 2 = 37°C and 3parts Ag + 3parts Cys; and 2A = 25°C and 3parts Ag + 3parts Cys. Black scale bar at bottom of figure = 10.5 cm.

Larger and smaller components of the self-assembled AgCysNPs could be separated in the pellet and supernatant, respectively, with a relative centrifugal force (rcf) of 2,500 for 10 minutes as shown in Figure 2.

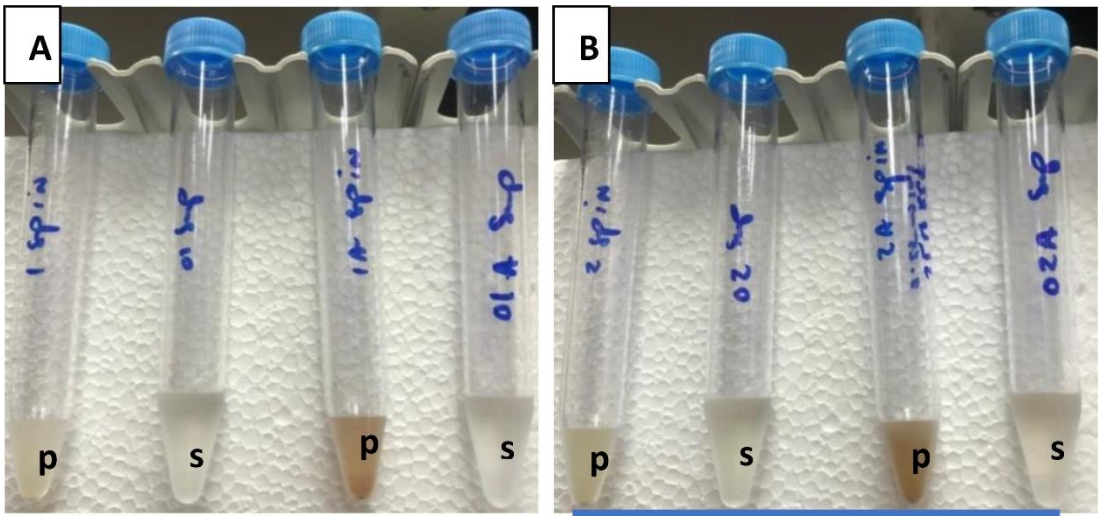

Figure 2 Separation of colloidal solutions of AgCysNPs. Solutions of AgCysNPs are shown in 15 ml tubes and were separated by centrifugation as described in methods. AgCysNPs as shown from left to right were generated under the following conditions in the indicated tubes: Figure 2A: 1 = 37°C and 2parts Ag + 2parts Cys; 1A = 25°C and 2parts Ag + 2parts Cys. Figure 2B: 2 = 37°C and 3parts Ag + 3parts Cys; and 2A = 25°C and 3parts Ag + 3parts Cys. Tubes labelled "p" indicate the centrifuged pellet for each condition, and those labelled "s" indicate the corresponding supernatant. Blue scale bar at bottom of Figure 2B indicates 14.5 cm.

Dynamic light scattering (DLS) analysis demonstrated distinct populations of generated AgCysNPs under the different conditions and in the centrifuged pellets vs. isolated supernatants as indicated in Figure 3. As expected, supernatants contained much smaller nanoparticles than found in the pellets. As we described previously [1], inclusion of HCl also resulted in silver nanoparticles with average diameter of 30 nm (AgCys-HCl in Figure 3).

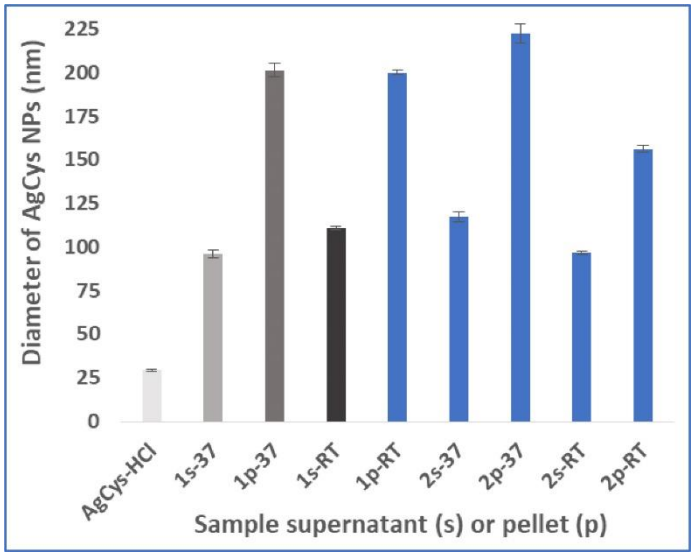

Figure 3 Dynamic Light Scattering (DLS) analysis of isolated AgCysNPs. AgCysNPs were synthesized at 37°C (-37) and room temperature (-RT), and separated into supernatants (s) and pellets (p) by centrifugation as described in methods. Grey/dark bars (series 1) were synthesized with 2 parts Ag + 2 parts cys as described in methods. In this group, AgCys-HCl included nanoparticles synthesized by including acid. Blue bars (series 2) were synthesized with 3 parts Ag + 3 parts cys. Data shown are an average of at least 3 runs per sample, with each run representing 13-16 determinations. Standard error bars are shown.

DLS has been used previously to characterize the average size of silver nanoparticles generated under different environmental conditions using gallic acid [11]. Here we showed that both 37°C and room temperature conditions could be successfully used to carry out green synthesis of silver nanoparticles (Figure 3). Scanning electron microscopy (SEM) was used to verify the nanoscale features of the synthesized silver nanoparticles Figure S1a, and EDAX analysis demonstrated the elemental presence of sulfur and silver, indicating the biohybrid nature of the material Figures S1b-d.

Generation of AgCysNPs under the different conditions may also be assessed optically using the formation of the coffee-ring effect [12, 13], as we have described previously to compare AgCysNPs vs. CuHARS [1]. Here we found that AgCysNPs generated under all conditions demonstrated a coffee-ring effect upon drying (Figure 4). Lower magnification of dried samples showing wider views of the coffee-ring effect are shown in Figure S2**.**

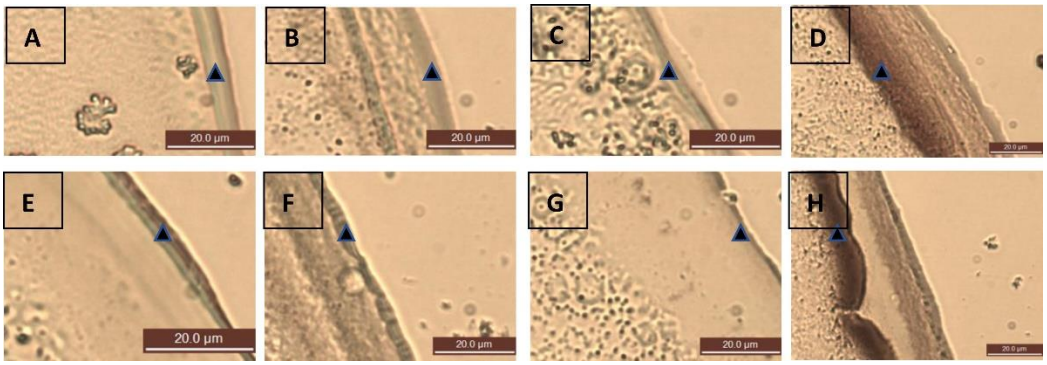

Figure 4 Coffee ring effect upon drying of AgCysNPs. All images are at 630x magnification with scale bar of 20 microns. Arrowheads indicate major coffee ring layers. Pellets of both room temperature conditions (4D and 4H) demonstrate the most color. Synthesis conditions = 37°C and 2parts Ag + 2parts Cys for supernatant (A) and pellet (B); 25°C and 2parts Ag + 2parts Cys for supernatant (C) and pellet (D); 37°C and 3parts Ag + 3parts Cys for supernatant (E) and pellet (F); and 25°C and 3parts Ag + 3parts Cys for supernatant (G) and pellet (H).

Spectrophotometry revealed a slight shift in absorbance values for the different silver:cystine ratios, and for 37°C and 25°C synthesis conditions (Figure 5). Khalkho et al. reported an absorbance peak of 390 nm for silver nanoparticles generated with the assistance of the amino acid cysteine [14]. In contrast, here, we found that when using the dimer of the amino acid, cystine for MOBs synthesis, that absorbance at 390 nm and in general, was greater for room temperature (25°C) synthesis conditions (samples 01A and 02A) than for 37°C synthesis (samples 1 and 2). No specific peak was observed, but rather a broad, generalized increase in absorbance with decreasing wavelength, consistent with what was reported previously [15], demonstrating a strong increase in the range of 400-200 nm where cystine absorbs.

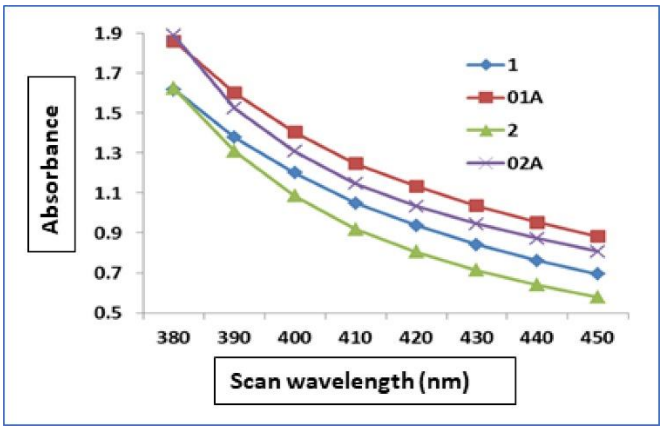

Figure 5 Absorbance scanning of AgCysNPs. Nanoparticles were scanned from 380-450 nm, as indicated and as described in Methods. Sample 1 = synthesis at 37°C with a ratio of silver:cystine of 2 + 2; 1A = the same ratio carried out at 25°C. Sample 2 = synthesis at 37°C with a ratio of silver:cystine of 3 + 3; 2A = the same ratio carried out at 25°C. Samples synthesized at 37°C (1 and 2), remained in a darkened oven during synthesis; samples synthesized at 25°C (1A and 2A) remained exposed to ambient light during synthesis.

When comparing the concentration of the dimer cystine used here to the amino acid cysteine in the thiolated form (dissolved in NaOH), we found differences in absorbance spectra as shown (Figure S3A) and consistent with prior results comparing these two sulfur-containing amino acids [16]. However, when scanning the prepared AgCysNPs after 3 cycles of washing with water and centrifugation, we did not detect any distinct peaks (800-200 nm), although some shoulder regions in the scans did emerge (Figure S3B).

Considering the light sensitivity of silver salts and silver nanoparticles [17, 18], we hypothesized that darker AgCysNPs product generated at room temperature as seen in Figure 1, Figure 2, and Figure 4, may have been due to exposure to ambient light during the synthesis. Room temperature synthesis was not carried out in a darkened oven, while 37°C synthesis was carried out in a darkened oven. We therefore carried out identical synthesis conditions using a darkened 37°C oven and one maintained at room temperature (25°C). Under these conditions, we found that identical ratios of silver to cystine resulted in similar colored solutions at 37°C and 25°C, with notable loss of the darker product at room temperature (Figure S4). In fact, compared to conditions where room temperature synthesis occurred in the presence of light (Figure 1), room temperature synthesis in a darkened oven resulted in lighter colored solutions than the 37°C condition (Figure S4).

3.2 Combined Synthesis of Mobs

We have previously described the self-assembly of MOBs separately for copper [10, 19] or silver [1], but never with both metals in the same assembly vessel. Figure 6 shows our first demonstration of self-assembly synthesis using copper and silver in the same vessel, carried out at 37°C and 25°C as indicated.

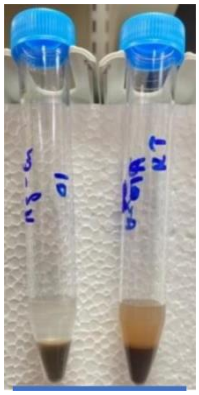

Figure 6 Synthesis of Ag- and Cu-MOBs in the same vessel. AgCysNPs and CuHARS were self-assembled in the same synthesis vessels (flasks), as described in Methods. Materials were then harvested and centrifuged in 15 ml tubes as described in Methods and resuspended in 1.5 ml of sterile water. Synthesis of materials in Tube on left was carried out at 37°C, and tube on right at 25°C. Synthesis conditions were 3 + 1 + 3 for Ag:Cu:Cystine as described in Methods. Blue scale bar at bottom of figure = 7.25 cm.

A difference in color is noted in the products produced simultaneously, with silver and copper co-synthesis at room temperature resulting in a darker (reddish) color for both pellet and supernatant, and synthesis at 37°C resulting in a brown pellet with more yellow colloidal

supernatant. Coffee ring drying of the copper and silver co-synthesis revealed a mixture of silver particulates and high-aspect ratio copper materials (Figure 7). In addition to the separation of materials by shape and drying pattern, here we observed in the copper/silver mixture, a clear polarization pattern which we have previously described only in pure CuHARS samples [1]. Due to size and shape, the polarizing materials are consistent with CuHARS, whereas the AgCysNPs are non-polarizing.

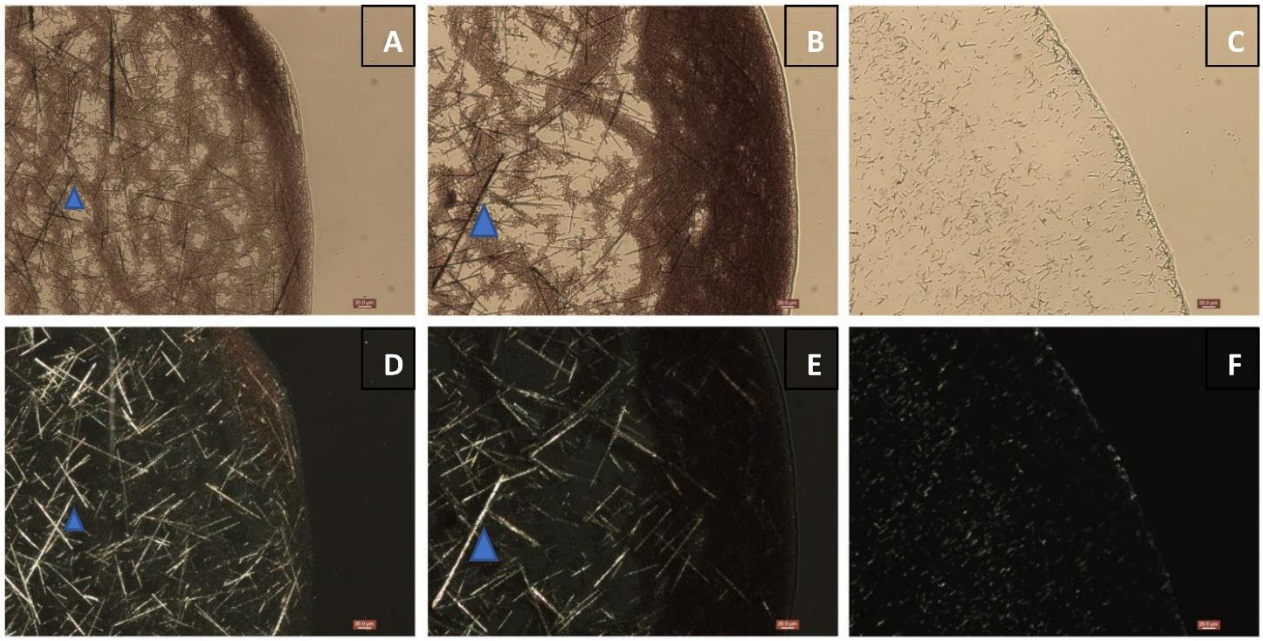

Figure 7 Coffee ring formation of AgCysNPs/CuHARS combination with brightfield images shown on top row, and corresponding polarization images on the bottom row. Samples synthesized at 37°C are shown in panels **A&D**, and samples synthesized at 25°C are shown in panels **B&E**. Synthesis conditions were 3 + 1 + 3 for Ag:Cu:Cystine (Panels **A + D** and **B + E**), and 1 + 1 for Cu:Cys (Panels **C + F**), as described in Methods. Panels **C&F** show pure CuHARS samples for comparative purposes. Scale bar indicated in all images = 20 microns. Prominent CuHARS in both brightfield and polarization images are indicated by blue arrowheads.

3.3 Cobalt Mob Synthesis

In addition, for the first time, we carried out combined cobalt and copper MOBs synthesis using cobalt sulfate. Synthesis was carried out as indicated at 37°C and 25°C, and resulted in distinct, whitish-colored products (Figure 8), with 37°C synthesis conditions resulting in a darker product compared to room temperature.

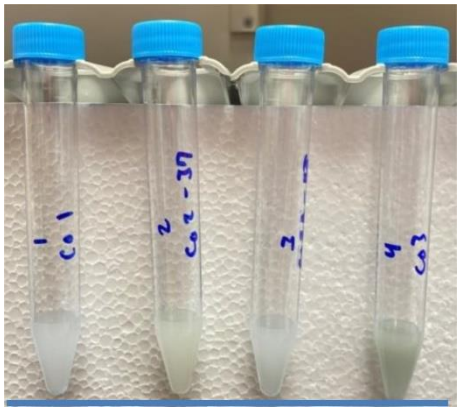

Figure 8 Combined Co- and Cu-MOBs synthesis at 37°C and 25°C. Cobalt and Copper MOBs were synthesized simultaneously in the same vessel as described in methods at 37°C or at room temperature (Tube 3), as indicated. Generated product was centrifuged and the obtained pellet resuspended in 1.5 ml sterile water as described in methods. Synthesis conditions were as follows in tubes from left to right using ratios as defined in Methods: Tube 1 = 1 + 1 + 2 for Co:Cu:Cys; Tube 2 = 2 + 1 + 2 for Co:Cu:Cys; Tube 3 = 2 + 1 + 2 for Co:Cu:Cys and carried out at room temperature; Tube 4 = 2 + 2 + 4 for Co:Cu:Cys. Blue scale bar at bottom of figure = 14.5 cm.

As was done for the combination of silver and copper samples, the combined cobalt and copper samples were applied to microscope slides for coffee-ring analysis and the cobalt MOBs were shown to be particulate and non-polarizing, whereas CuHARS were elongated and polarizing (Figure 9).

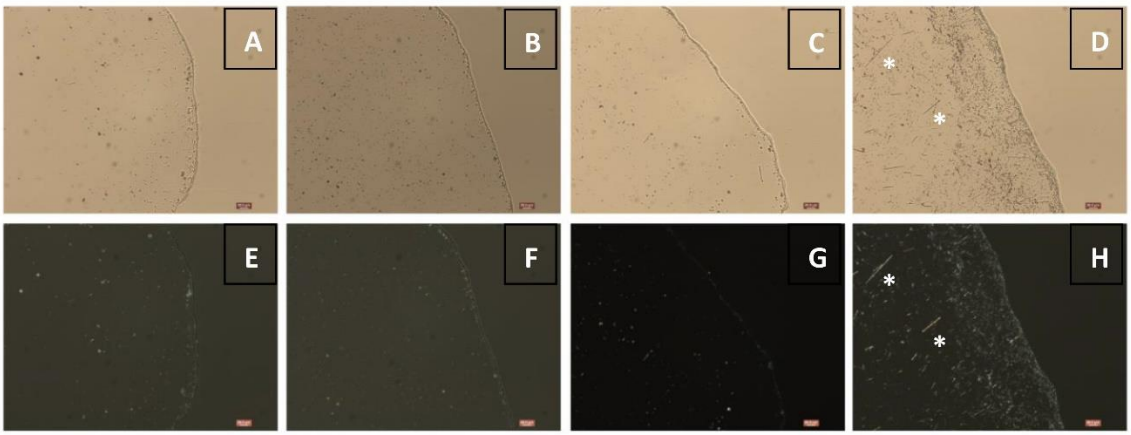

Figure 9 Coffee-ring formation of copper/cobalt co-synthesis. Copper and Cobalt MOBs were co-synthesized as described in methods and then 4 µl applied to a microscope slide for coffee-ring analysis. Top row shows the brightfield images, and bottom row shows the polarization images of each corresponding sample. Synthesis conditions were as follows using ratios as defined in Methods and carried out at 37°C except for Panels **C&G** as indicated. Panels **A&E** = 1 + 1 + 2 for Co:Cu:Cys; **B&F** = 2 + 1 + 2 for Co:Cu:Cys; **C&G** = 2 + 1 + 2 for Co:Cu:Cys and carried out at room temperature; and **D&H** = 2 + 2 + 4 for Co:Cu:Cys. Scale bar indicates 20 microns for all images. Prominent CuHARS are indicated by white asterisks.

It was interesting to note that under conditions of 37°C vs room temperature, cobalt nanoparticles were favored (Figure 9B&F). In contrast, under the same component ratios, CuHARS only appeared when green synthesis was carried out at room temperature (Figure 9C&G and S5). Increasing all synthesis components resulted in the greatest amount of material for both cobalt and copper when carried out at 37°C (Figure 9D&H). In this preliminary work describing CoMOBs for the first time, cobalt particles formed ranged from nanoscale to microscale (Figure S6a). Elemental analysis of the generated CoMOBs indicated a biohybrid with both cobalt and sulfur appearing as prominent components of the material (Figure S7). MOBs generated using copper (CuHARS), scale from the nano- to the micro-, as we have previously shown [10], with nanoscale diameters and microscale length and were also shown in the same sample synthesizing copper and cobalt MOBs simultaneously (Figure S6). EDX analysis of CuHARS demonstrated sulfur and copper self-assembling as a biohybrid, with sulfur coming from the amino acid dimer cystine, combining with the non-biological metal component of copper [10], and as shown here when synthesized simultaneously with cobalt (Figure S8).

While green synthesis methods have been described to generate silver nanoparticles using the amino acid cysteine [14, 20], these techniques also included sodium citrate and/or sodium borohydride in the mixture to form the nanoparticles. In contrast, our green synthesis method simply used silver sulfate and the amino acid dimer cystine for the nanoparticle synthesis. We used this same approach to generate cobalt MOBS simultaneously with CuHARS, and the particles were formed both at room temperature and at 37°C. Green synthesis of cobalt oxide nanoparticles has been reported previously, using different starting cobalt materials than here [21, 22]. However, although both of these manuscripts reported green synthesis due to use of plant extracts, the synthesis procedures in both cases involved elevated temperatures of 75°C [21] or higher [22], while our work carried out all synthesis at room temperature or 37°C for comparative purposes.

Along with our previous report of copper and silver MOBs [1], the work shown here indicates that cobalt may also be added to the family, which we now name cobalt MOBs (CoMOBs). CoMOBs as isolated here using green synthesis methods could have future applications interest as a potentially magnetically susceptible material [23, 24]. In our green synthesis method combining copper and cobalt, we found that the resulting material was susceptible to an external magnetic field (Figure 10a and 10d).

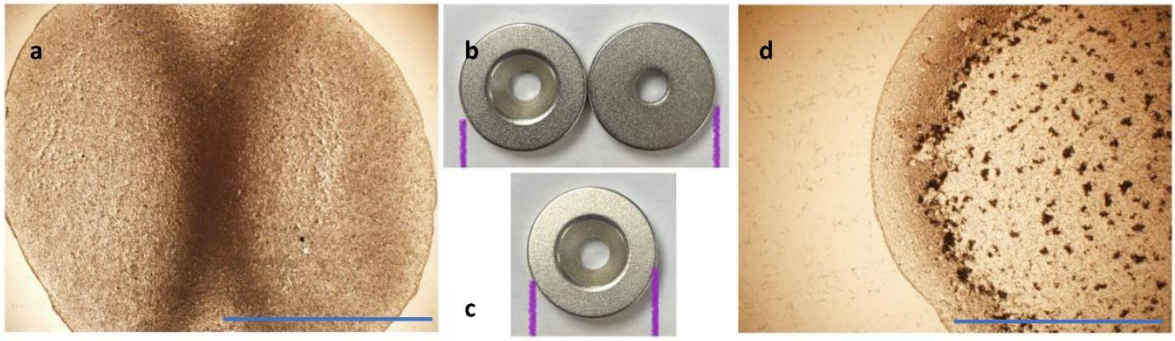

Figure 10 Magnetic susceptibility of CoMOBs. Cobalt and copper containing MOBs were synthesized and exposed to a magnetic field as described in methods. A 20 µl sample of Co/Cu MOBs mixture (**10a**), was placed on top of two ring magnets as shown (**10b**), and imaged using brightfield microscopy at 2x magnification. Sample in **10d** was identical Co/Cu MOBs mixture as shown in 10A, but diluted 2-fold in water, and then the 20 µl sample placed on top of a single ring magnet as shown in **10c**. Width of the two magnets as indicated by vertical purple lines = 2.5 cm for **10b** and 1.2 cm for **10c**. Scale bars in **10a** and **10d** = 3.3 mm.

4. Discussion

Green synthesis methods carried out at both 37°C and room temperature resulted in successful generation of silver nanoparticles using cystine (AgCysNPs). DLS analysis demonstrated average nanoparticle diameters of less than 100 nm (Figure 3), and less than 30 nm when including HCl in the green synthesis vessel as we have previously described [1]. In addition to comparing green synthesis results at 37°C and room temperature, we also varied the amount of metal precursors and cystine in the synthesis vessel. Here for two different concentrations of silver sulfate and cystine, we found that room temperature conditions gave a darker product with higher measured absorbance values (Figure 5). The darker material was due to exposure in the room temperature conditions to ambient light, as was shown when we carried out synthesis at 37°C and room temperature using a darkened oven for both conditions (Figure S4).

One aspect of green synthesis methods in the future might consider simultaneous generation of materials in the same vessel. We have previously shown the synthesis of copper MOBs and silver MOBs in separate vessels [1, 10]. Here for the first time we demonstrate that silver or cobalt may be combined with copper in the same vessel to create new MOBs. Once generated, the distinct size and shapes of copper, silver, and cobalt MOBs can aid in their isolation and identification: for example, CuHARs readily polarize light as shown under microscopy [1] and Figure 7. Previously, different nanostructures combining copper and other metals have been described using the co-precipitation technique [25-27], but this often involved high-temperature heating steps to destroy the organic component of materials used during synthesis [25, 26] or sequential doping steps without organic materials [27]. In our methods described here to generate MOBs, all steps were carried out at 37°C or below, and in this manner, organic materials such as cystine used in the synthesis were retained. Maintenance of physiologically permissive temperatures during green synthesis of nanomaterials may have advantages not only for biologically derived manufacturing components such as we have shown here for cystine, but also

for production of nanomaterials using intact biological entities and systems such as plants, fungus, bacteria, and yeast [28]. Although it was not optimized for such, our initial discovery of the self-assembly of CuHARS was made in an intact, physiologically maintained cell culture system [10], and was then simplified to isolate the essential biological component for the biohybrid, in this case the amino acid dimer cystine.

In the case of cobalt MOBs, magnetic susceptibility of the material can be utilized for identification and potential future applications (Figure 10). As shown, the mixed materials reflected patterns due to the ring magnets in two different configurations. In contrast, the same sample materials dried without a magnetic field did not show these patterns (Figure S9). It is anticipated that in the future, this magnetic susceptibility could provide a means for patterning individual or mixed MOBs materials.

We have confirmed that the synthesized materials contain organic ligand components, most likely, the starting amino acid dimer cystine and/or the monomer amino acid form, cysteine [10]. This was verified for multiple forms of the MOBs. For copper, we showed that CuHARS could be formed using copper nanoparticles or copper sulfate. Upon elemental analysis, CuHARS generated from both copper starting materials included sulfur, which was not found in the copper nanoparticle starting material used [10]. Therefore, sulfur in the stable CuHARS formed is most likely in the form of sulfur-containing cystine or cysteine, used during the synthesis. Further support of organic ligand components in CuHARS comes from the presence and increase in carbon and nitrogen peaks in the stable biohybrid compared to the starting materials [10]. Elemental analysis of AgCysNPs and CoMOBs is also consistent with the presence of organic ligand components (Figures S1, S7, and S8), and due to the particulate nature of both AgCysNPs and CoMOBs, the organic ligand components indicated by the presence of sulfur and carbon is consistent with a capping/stabilization action by the cystine or cysteine used in the synthesis. Cysteine has been used to synthesize stabilized silver nanoparticles [29] and cobalt-iron nanoparticles [30], but to our knowledge, the current work is the first to use the dimer cystine as a stabilizing agent.

The mechanism(s) for the green synthesis of copper, silver, and cobalt metal-organic biohybrids (MOBs) is not known at this time. However, the oxidation states of copper and cobalt used here were in the +2 state at the beginning of synthesis, and all metal salts were in the sulfate form. Copper, having possible oxidation states of +2 and +1, is known to bind to cystine and cysteine [31, 32], and under the reducing conditions of sodium hydroxide used here [10], cystine or cysteine could bind to copper via deprotonated carboxylate groups [33]. This could lead to a $Cu(Cys)_2$ form, as suggested for cysteine [33]. Here, since we utilized cystine, a $Cu(Cys)_2$ with Cys being the dimer cystine, could provide a mechanism whereby CuHARS are formed and generate the highly elongated (high-aspect ratio) structures we have shown. However, since cystine also contains sulfur, if thiol groups are deprotonated as is suggested for cysteine [33], copper binding to sulfur may be preferred over carboxylate. Thus, we suggest here a mechanism for CuHARS formation whereby copper competes with both sulfur and carboxylate groups of cystine, and this provides length (elongation), and width (3-dimensionality) for the growing CuHARS. Recently, lysine hydrochloride-Cu(II) complexes were described that were generated using the liquid-phase synthesis method [34]. While the generation of these lysine-copper complexes included assisted heating at 70°C, followed by precipitation at room temperature [34], it may be of interest in future

studies to replace cystine with lysine using our MOBs methods, under conditions of strictly physiological (37°C), or lower temperatures.

The formation of MOBs using the metals silver and cobalt combined with cystine result in particulate forms, rather than the elongated CuHARS of copper. This may be due to the +1 oxidation state for silver, whereby cystine provides a stabilizing and capping function, surrounding a core of silver to form nanoparticles [35]. The bio-reducing capabilities of many compounds extracted from biologicals has been previously reported for generating silver nanoparticles [36, 37]. Here we were successful in generating silver nanoparticles using the amino acid dimer cystine.

In contrast to copper and silver, cobalt has oxidation states of +2 or +3, and has been shown to bind strongly to the sulfur atoms of cysteines in observed and computational studies; oxidation phenomena leading to Co(III) in free or complexed form were never observed in these studies [38]. Thus, cobalt under our conditions resulted in large particulates, likely capped by the cystine, or the breakdown product of cysteine [30]. It therefore remains likely that for both silver and cobalt, under the conditions used here for MOBs self-assembly, cystine serves as a stabilizing/capping agent [39], whereas for copper it serves as a linker, providing an elongation factor that results in high-aspect ratio copper MOBs.

5. Conclusions

We demonstrated here for the first time that MOBs could be co-synthesized in the same vessel using two combinations: 1) copper and silver, and 2) copper and cobalt. Due to the light polarization properties of CuHARS, co-synthesis of MOBs which include copper may be separated on the basis of size and shape of the materials obtained, and verified using light polarization and digital microscopy as we have shown here. This facile green synthesis of multiple types of nanomaterials in the same vessel may further advance the benefits of self-assembly using minimal energy. Our green synthesis methods generated microscale and nanoscale materials at both 37°C and at room temperature, providing a smaller energy footprint for nanomaterials production. In one case, where cobalt and copper were combined in the same vessel, temperature differences contributed to selective green synthesis of cobalt particles alone (at 37°C), vs. a mixture of cobalt particles and CuHARS, which occurred at room temperature. Thus under the conditions carried out here, modest temperatures in the range of 37°C-room temperature, may be used to selectively produce different types of nanomaterials using green synthesis.

Acknowledgments

The authors would like to thank Ms. Shaylee Boudreaux for assistance with microscopy imaging in this work and Mr. Davis Bailey for assistance with electron microscopy.

Author Contributions

N.U. carried out experiments, characterized materials, and provided technical details for the text. K.M. characterized materials, conceptualized experiments, and provide background information for the text. T.K. characterized materials and provided technical details for the text. M.D. conceptualized all experiments, assisted with characterization of materials, provided technical details for the text, and wrote the manuscript with input from other co-authors.

Funding

This work was supported by the Louisiana Board of Regents Proof-of-Concept/Prototyping Initiative program [LEQSF(2021-22)-RD-D-05].

Competing Interests

The authors have declared that no competing interests exist.

Additional Materials

The following additional materials are uploaded at the page of this paper.

1. Figure S1: Scanning electron microscopy analysis of silver nanoparticles.
2. Figure S2: Coffee ring effect upon drying of AgCysNPs.
3. Figure S3: Absorbance of amino acid monomer cysteine vs. dimer cystine and AgCysNPs.
4. Figure S4: AgCysNPs synthesized under darkened conditions.
5. Figure S5: Comparative generation of MOBs types at 37°C vs room temperature.
6. Figure S6: Scanning electron microscopy images of cobalt MOBs and CuHARS
7. Figure S7: Energy dispersive X-ray spectroscopy (EDX) analysis of cobalt and copper MOBs-Sample high in CoMOBs %.
8. Figure S8: Energy dispersive X-ray spectroscopy (EDX) analysis of cobalt and copper MOBs-Sample high in CuHARS %.
9. Figure S9: Drying pattern of Cobalt/Copper MOBs without magnetic field (controls).

References

1. Karekar N, Karan A, Khezerlou E, Prajapati N, Pernici CD, Murray TA, et al. Self-Assembled metal-organic biohybrids (MOBs) using copper and silver for cell studies. Nanomaterials. 2019; 9: 1282. PMID: 31500351.
2. Wang X, Li X, Liu D, Song S, Zhang H. Green synthesis of Pt/CeO_2/graphene hybrid nanomaterials with remarkably enhanced electrocatalytic properties. Chem Commun. 2012; 48: 2885-2887.
3. Galstyan V, Poli N, D'Arco A, Macis S, Lupi S, Comini E. A novel approach for green synthesis of WO_3 nanomaterials and their highly selective chemical sensing properties. J Mater Chem. 2020; 8: 20373-20385.
4. Suramwar NV, Thakare SR, Khaty NT. One pot synthesis of copper nanoparticles at room temperature and its catalytic activity. Arab J Chem A. 2016; 9: S1807-S1812.
5. Cao Y, Jia D, Hu P, Wang R. One-step room-temperature solid-phase synthesis of $ZnFe_2O_4$ nanomaterials and its excellent gas-sensing property. Ceram Int. 2013; 39: 2989-2994.
6. Huq MA. Green synthesis of silver nanoparticles using Pseudoduganella eburnea MAHUQ-39 and their antimicrobial mechanisms investigation against drug resistant human pathogens. Int J Mol Sci. 2020; 21: 1510.
7. Li G, He D, Qian Y, Guan B, Gao S, Cui Y, et al. Fungus-mediated green synthesis of silver nanoparticles using Aspergillus terreus. Int J Mol Sci. 2011; 13: 466-476.

8. Banerjee P, Satapathy M, Mukhopahayay A, Das P. Leaf extract mediated green synthesis of silver nanoparticles from widely available Indian plants: Synthesis, characterization, antimicrobial property and toxicity analysis. Bioresour Bioprocess. 2014; 1: 1-10.
9. Kumar R, Ghoshal G, Jain A, Goyal M. Rapid green synthesis of silver nanoparticles (AgNPs) using (Prunus persica) plants extract: Exploring its antimicrobial and catalytic activities. J Nanomed Nanotechnol. 2017; 8: 1-8.
10. Cotton Kelly K, Wasserman JR, Deodhar S, Huckaby J, DeCoster MA. Generation of scalable, metallic high-aspect ratio nanocomposites in a biological liquid medium. J Vis Exp. 2015: E52901.
11. Martínez-Castañon GA, Nino-Martinez N, Martinez-Gutierrez F, Martinez-Mendoza JR, Ruiz F. Synthesis and antibacterial activity of silver nanoparticles with different sizes. J Nanopart Res. 2008; 10: 1343-1348.
12. Yunker PJ, Still T, Lohr MA, Yodh AG. Suppression of the coffee-ring effect by shape-dependent capillary interactions. Nature. 2011; 476: 308-311. PMID: 21850105.
13. Crivoi A, Duan F. Elimination of the coffee-ring effect by promoting particle adsorption and long-range interaction. Langmuir. 2013; 29: 12067-12074.
14. Khalkho BR, Kurrey R, Deb MK, Shrivas K, Thakur SS, Pervez S, et al. L-cysteine modified silver nanoparticles for selective and sensitive colorimetric detection of vitamin B1 in food and water samples. Heliyon. 2020; 6: E03423.
15. Rigo A, Corazza A, di Paolo ML, Rossetto M, Ugolini R, Scarpa M. Interaction of copper with cysteine: Stability of cuprous complexes and catalytic role of cupric ions in anaerobic thiol oxidation. J Inorg Biochem. 2004; 98: 1495-1501.
16. Middendorf TR, Aldrich RW, Baylor DA. Modification of cyclic nucleotide-gated ion channels by ultraviolet light. J Gen Physiol. 2000; 116: 227-252. PMID: 10919869. PMCID: 2229495.
17. Olfati A, Kahrizi D, Balaky ST, Sharifi R, Tahir MB, Darvishi E. Green synthesis of nanoparticles using Calendula officinalis extract from silver sulfate and their antibacterial effects on Pectobacterium caratovorum. Inorg Chem Commun. 2021; 125: 108439.
18. Korchev A, Bozack MJ, Slaten BL, Mills G. Polymer-initiated photogeneration of silver nanoparticles in SPEEK/PVA films: Direct metal photopatterning. J Am Chem Soc. 2004; 126: 10-11.
19. Deodhar S, Huckaby J, Delahoussaye M, DeCoster MA. High-aspect ratio bio-metallic nanocomposites for cellular interactions. IOP Conf Ser: Mater Sci Eng. 2014; 64: 012014.
20. Zhang W, Zhang L, Sun Y. Size-controlled green synthesis of silver nanoparticles assisted by L-cysteine. Front Chem Sci Eng. 2015; 9: 494-500.
21. Bibi I, Nazar N, Iqbal M, Kamal S, Nawaz H, Nouren S, et al. Green and eco-friendly synthesis of cobalt-oxide nanoparticle: Characterization and photo-catalytic activity. Adv Powder Technol. 2017; 28: 2035-2043.
22. Hafeez M, Shaheen R, Akram B, Haq S, Mahsud S, Ali S, et al. Green synthesis of cobalt oxide nanoparticles for potential biological applications. Mater Res Express. 2020; 7: 025019.
23. Rutnakornpituk M, Thompson MS, Harris LA, Farmer KE, Esker AR, Riffle JS, et al. Formation of cobalt nanoparticle dispersions in the presence of polysiloxane block copolymers. Polymer. 2002; 43: 2337-2348.

24. Bönnemann H, Brijoux W, Brinkmann R, Matoussevitch N, Waldöfner N, Palina N, et al. A size-selective synthesis of air stable colloidal magnetic cobalt nanoparticles. Inorganica Chim Acta. 2003; 350: 617-624.
25. Pramothkumar A, Senthilkumar N, Jothivenkatachalam K. Flake-like $CuMn_2O_4$ nanoparticles synthesized via co-precipitation method for photocatalytic activity. Physica B Condens Matter. 2019; 572: 117-124.
26. Ghaani M, Saffari J. Synthesis of CuFe2 O4 Nanoparticles by a new co-precipitation method and using them as Efficient Catalyst for One-pot Synthesis of Naphthoxazinones. J Nanostructures. 2016; 6: 172-178.
27. Naz G, Shabbir M, Ramzan M, Haq BU, Arshad M, Tahir MB, et al. Synergistic effect of Cu_x/Mg_x and $Zn_{1-x}O$ for enhanced photocatalytic degradation and antibacterial activity. Physica B Condens Matter. 2022; 624: 413396.
28. Hasan M, Ullah I, Zulfiqar H, Naeem K, Iqbal A, Gul H, et al. Biological entities as chemical reactors for synthesis of nanomaterials: Progress, challenges and future perspective. Mater Today Chem. 2018; 8: 13-28.
29. Diamai S, Negi DP. Cysteine-stabilized silver nanoparticles as a colorimetric probe for the selective detection of cysteamine. Spectrochim Acta Part A. 2019; 215: 203-208.
30. Wang G, Zhou F, Li X, Li J, Ma Y, Mu J, et al. Controlled synthesis of L-cysteine coated cobalt ferrite nanoparticles for drug delivery. Ceram Int. 2018; 44: 13588-13594.
31. Arathi PJ, Seemesh B, Ramanathan V. Disulphide linkage: To get cleaved or not? Bulk and nano copper based SERS of cystine. Spectrochim Acta Part A. 2018; 196: 229-232.
32. Dokken KM, Parsons JG, McClure J, Gardea-Torresdey JL. Synthesis and structural analysis of copper (II) cysteine complexes. Inorg Chim Acta. 2009; 362: 395-401.
33. Ramek M, Pejić J, Sabolović J. Structure prediction of neutral physiological copper (II) compounds with L-cysteine and L-histidine. J Inorg Biochem. 2021; 223: 111536.
34. Wu Z, Fu Z, Tian Y, Hasan M, Huang L, Yang Y, et al. Fabrication and characterization of lysine hydrochloride Cu (ii) complexes and their potential for bombing bacterial resistance. Green Process Synth. 2022; 11: 445-457.
35. Ditta SA, Yaqub A, Ullah R, Tanvir F. Evaluation of amino acids capped silver nanoconjugates for the altered oxidative stress and antioxidant potential in albino mice. J Mater Res. 2021; 36: 4344-4359.
36. Hasan M, Teng Z, Iqbal J, Awan U, Meng S, Dai R, et al. Assessment of bioreducing and stabilizing potential of Dragon's blood (Dracaena cochinchinensis, Lour. SC Chen) resin extract in synthesis of silver nanoparticles. Nanosci Nanotechnol Lett. 2013; 5: 780-784.
37. Zulfiqar H, Zafar A, Rasheed MN, Ali Z, Mehmood K, Mazher A, et al. Synthesis of silver nanoparticles using Fagonia cretica and their antimicrobial activities. Nanoscale Adv. 2019; 1: 1707-1713.
38. Buchmann W, Spezia R, Tournois G, Cartailler T, Tortajada J. Structures and fragmentations of cobalt (II)–cysteine complexes in the gas phase. J Mass Spectrom. 2007; 42: 517-526.
39. Vishnevetskii DV, Mekhtiev AR, Perevozova TV, Ivanova AI, Averkin DV, Khizhnyak SD, et al. l-Cysteine as a reducing/capping/gel-forming agent for the preparation of silver nanoparticle composites with anticancer properties. Soft Matter. 2022; 18: 3031-3040.

Enjoy *Recent Progress in Materials* by:

1. Submitting a manuscript
2. Joining in volunteer reviewer bank
3. Joining Editorial Board
4. Guest editing a special issue

For more details, please visit:
http://www.lidsen.com/journals/rpm